Cancer Immunol Immunother (2015) 64:1407–1417
DOI 10.1007/s00262-015-1742-0

ORIGINAL ARTICLE

Immunosuppressive activity of cancer-associated fibroblasts in head and neck squamous cell carcinoma

Hideyuki Takahashi[1] · Koichi Sakakura[1] · Reika Kawabata-Iwakawa[2] · Susumu Rokudai[3] · Minoru Toyoda[1] · Masahiko Nishiyama[3] · Kazuaki Chikamatsu[1]

Received: 8 January 2015 / Accepted: 10 July 2015 / Published online: 23 July 2015

Abstract Cancer-associated fibroblasts (CAFs) have been shown to play an important role in angiogenesis, invasion, and metastasis. In the present study, we determined whether CAFs within the tumor microenvironment (TME) in head and neck squamous cell carcinoma (HNSCC) contributed to promoting immunosuppression and evasion from immune surveillance. Six pairs of CAFs and normal fibroblasts (NFs) were established from the resected tumor tissues of patients with HNSCC. The effects of CAFs and NFs on the functions of T cells were comparatively analyzed. CAFs expressed the co-regulatory molecules, B7H1 and B7DC, whereas NFs did not. The expression levels of cytokine genes, including those for *IL6*, *CXCL8*, *TNF*, *TGFB1*, and *VEGFA*, were higher in CAFs. T cell proliferation was suppressed more by CAFs or their supernatants than by NFs. Moreover, PBMCs co-cultured with the supernatants of CAFs preferentially induced T cell apoptosis and regulatory T cells over those co-cultured with the supernatants of NFs. A microarray analysis revealed that the level of genes related to the leukocyte extravasation and paxillin signaling pathways was higher in CAFs than in NFs. These results demonstrated that CAFs collaborated with tumor cells in the TME to establish an immunosuppressive network that facilitated tumor evasion from immunological destruction.

Keywords Cancer-associated fibroblasts · Head and neck squamous cell carcinoma · Immunosuppression · Regulatory T cells · T cell apoptosis

Abbreviations

7-ADD	7-Amino-actinomycin D
APC	Allophycocyanin
CAF	Cancer-associated fibroblast
CCL7	Chemokine ligand 7
CFSE	Carboxyfluorescein succinimidyl ester
Cy	Cyanine
FAP	Fibroblast activation protein
GAPDH	Glyceraldehyde-3-phosphate dehydrogenase
HGF	Hepatocyte growth factor
HNSCC	Head and neck squamous cell carcinoma
IGF	Insulin-like growth factor
IL	Interleukin
IPA	Ingenuity pathway analysis
MMP	Matrix metalloproteinase
NF	Normal fibroblast
NSCLC	Non-small cell lung cancer
SMA	Smooth muscle actin
TGF	Transforming growth factor
TME	Tumor microenvironment
Treg	Regulatory T cells
VEGF	Vascular endothelial growth factor

Introduction

Head and neck squamous cell carcinoma (HNSCC) is a fatal malignancy that accounts for approximately 650,000

✉ Kazuaki Chikamatsu
tikamatu@gunma-u.ac.jp

[1] Department of Otolaryngology-Head and Neck Surgery, Gunma University Graduate School of Medicine, 3-39-22, Maebashi, Gunma 371-8511, Japan

[2] Division of Integrate Oncology Research, Gunma University Initiative for Advanced Research, 3-39-22, Maebashi, Gunma 371-8511, Japan

[3] Department of Molecular Pharmacology and Oncology, Gunma University Graduate School of Medicine, 3-39-22, Maebashi, Gunma 371-8511, Japan

new patients every year. In spite of continual improvements in surgical techniques and the introduction of new chemotherapeutic agents and radiotherapy regimens, the five-year survival rate of HNSCC has remained unchanged for decades and is still 50 % [1, 2]. Therefore, further explorations of new therapeutic targets are needed in order to improve the prognosis and survival of patients with HNSCC.

Tumor tissue is composed not only of tumor cells, but also of various stromal cells, including fibroblasts, epithelial cells, endothelial cells, and immune cells, and these stroma cells contribute to tumor growth and progression. Recent findings revealed that cancer-associated fibroblasts (CAFs), one of the most abundant and active cellular components of the tumor stroma, played an important role in angiogenesis, invasion, and metastasis unlike normal fibroblasts (NFs) residing in healthy tissue [3–5].

The abundance of CAFs has been clinically correlated with poor prognosis in several malignancies, including lung [6] and colorectal cancers [7]. CAFs produce various cytokines and growth factors, such as transforming growth factor (TGF)-β, vascular endothelial growth factor (VEGF), interleukin (IL)-6 and IL-8, and insulin-like growth factor (IGF), and directly or indirectly influence the behavior of malignant cells through signaling pathways mediated by these molecules [8, 9]. Based on these findings, CAFs are considered to be active participants in the induction of immunosuppression and promotion of tumor evasion from immune surveillance. However, the immunological significance of CAFs in the tumor microenvironment (TME) is not yet fully understood.

Anti-tumor innate and adaptive immunity comprising the cancer immune surveillance network are generally designed to survey, recognize, and eliminate tumor cells. T cells predominantly orchestrate the host immune system, and the T cell infiltration of tumor lesions has been reported to correlate with improved prognoses in various types of cancers [10, 11]. However, anti-tumor immunity is often down-regulated with a developing tumor due to the expansion of regulatory T cells (Treg) as well as the production of immunosuppressive factors [12–14]. Thus, human tumors are known to employ various immunosuppressive mechanisms to evade the anti-tumor activities of immune cells, and tumor evasion from immunological destruction has recently emerged as one of the hallmarks of cancer [15].

In the present study, we investigated whether CAFs within the TME contributed to tumor evasion in HNSCC which are known to be highly immunosuppressive [16]. After establishing six pairs of CAFs and NFs from the resected tumor tissues of patients with HNSCC, we performed a comparative analysis of CAFs and NFs to evaluate their ability to regulate the functions of T cells. Our results have provided novel insights into immunosuppressive mechanisms in the TME and suggest that novel therapeutic approaches targeting CAFs may benefit patients with HNSCC.

Materials and methods

Patient samples

Tumor tissues and their normal counterparts were obtained from six newly diagnosed HNSCC patients (3 oral cavity cancer and 3 hypopharyngeal cancer patients) who underwent surgery at the Department of Otolaryngology, Head and Neck Surgery, Gunma University Hospital. The normal counterparts were defined by the non-cancerous region at least 2 cm away from the tumor margin. Patients received no anticancer drugs or radiotherapy before surgery. All tumors were obtained according to the protocol, which was approved by the Institutional Review Board of Gunma University. All patients provided written informed consent. The tissue was soaked in DMEM (Gibco, Grand Island, NY) supplemented with 1000 units/ml penicillin, 1000 μg/ml streptomycin, and 2.5 μg/ml fungizone (all reagents from Gibco) for 4 h, and then washed with DMEM supplemented with 10 % FCS, 100 units/ml penicillin, and 100 μg/ml streptomycin (henceforth referred to as "conditioned DMEM"). The tissue was sliced into 1- to 3-mm^3 pieces under sterile conditions. These fragments were transferred into a six-well plate with conditioned DMEM. Half of the medium was changed once or twice a week thereafter. After the sufficient outgrowth of cells, fibroblasts were removed by a treatment with TrypLE™ Express Enzyme (Gibco) and seeded into tissue culture flasks. They were analyzed by flow cytometry or real-time quantitative reverse transcription polymerase chain reaction (RT-PCR) after the sufficient outgrowth of cells. All CAFs and NFs used in this study were from less than 10 passages. Culture supernatants were collected from semi-confluent cultures 72 h after the medium was changed and then centrifuged and stored at −80 °C until use.

Peripheral blood mononuclear cells

Peripheral blood mononuclear cells (PBMCs) were prepared from healthy donor blood by density gradient centrifugation on a Ficoll-Paque PLUS (GE Healthcare, Pittsburgh PA). They were stored at −80 °C until use.

Flow cytometry analysis of primary fibroblast cultures

Fibroblasts were stained with the following mouse anti-human antibodies to define the expression of fibroblast surface markers, HLA molecules, or co-regulatory molecules:

phycoerythrin (PE)-CD11b/Mac-1, PE-CD34, PE-CD45, PE-CD90/Thy-1, PE-α-smooth muscle actin (α-SMA) (all reagents from R&D Systems, Minneapolis, MN), PE-HLA class I, PE-HLA-DR, PE-CD80/B7-1, PE-CD86/B7-2, PE-B7H1/PD-L1, PE-B7DC/PD-L2, or PE-B7H3 (all reagents from eBioscience, San Diego, CA), and fibroblast activation protein (FAP; unconjugated; R&D Systems). A PE-conjugated goat anti-mouse monoclonal antibody (mAb; BD Pharmingen) was used as a secondary antibody for FAP staining. A Cytofix/Cytoperm™ Kit (BD Bioscience, San Jose, CA) was used to perform intracellular staining for PE-α-SMA. Respective immunoglobulin G (IgG) isotype-matched controls (BD Bioscience) were used as negative controls. Flow cytometry was conducted using a FACSCalibur flow cytometer (BD Bioscience), and data analysis was performed with FlowJo software (TreeStar, Ashland, OR).

Real-time qRT-PCR

Total RNA was extracted using an RNeasy mini kit (Qiagen, Valencia, CA). Quantitative RT-PCR was performed in triplicate using a Power SYBR Green RNA-to-CT 1-Step Kit on an Applied Biosystems StepOne (Applied Biosystems, Foster City, CA). The melting curve was recorded at the end of every run to assess product specificity. Glyceraldehyde-3-phosphate dehydrogenase (*GAPDH*) was used as an internal control gene. Relative expression levels were determined by the $2^{-\Delta\Delta C_t}$ method, in which Ct represented the threshold cycle.

The PCR primers used in this study were as follows: *IL6* forward primer, 5′-AAGCCAGAGCTGTGCAGA TGAGTA-3′, reverse primer, 5′-TGTCCTGCAGCCACT GGTTC-3′; *CXCL8* forward primer, 5′-GTGCAGAGG GTTGTGGAGAAGTTT-3′, reverse primer, 5′-TCACTGG CATCTTCACTGATTCTTG-3′; *IL10* forward primer, 5′-GAGATGCCTTCAGCAGAGTGAAGA-3′, reverse primer, 5′-AGGCTTGGCAACCCAGGTAAC-3′; *TNF* forward primer, 5′-TGCTTGTTCCTCAGCCTCTT-3′, reverse primer, 5′-CAGAGGGCTGATTAGAGAGAG GT-3′; *VEGFA* forward primer, 5′-ACTTCCCCAAATCA CTGTGG-3′, reverse primer, 5′-GTCACTCACTTTGCCC CTGT-3′; *TGFB1* forward primer, 5′-AGCGACTCGCC AGAGTGGTTA-3′, reverse primer, 5′-GCAGTGTGTT ATCCCTGCTGTCA-3′; *FOXP3* forward primer, 5′-GTTCACACGCATGTTTGCCTTC-3′, reverse primer, 5′-GCACAAAGCACTTGTGCAGACTC-3′, and *GAPDH* forward primer, 5′-GCACCGTCAAGGCTGAGAAC-3′; reverse primer, 5′-ATGGTGGTGAAGACGCCAGT-3′.

Carboxyfluorescein succinimidyl ester (CFSE)-based suppression assay

Healthy donor PBMCs were incubated with 1.5 μM CFSE (Molecular Probe/Invitrogen) for 15 min at 37 °C and quenched with ice-cold FBS. After 5 min at room temperature in the dark, they were centrifuged and washed a further three times. CFSE-labeled PBMCs (1×10^5) were plated into 96-well plates in the presence of CAFs or NFs ($2.5x10^4$) or culture supernatants from CAFs or NFs (half-diluted with conditioned RPMI 1640 medium). An anti-CD3/anti-CD28 stimulus (Treg Suppression Inspector human; Miltenyi Biotec, Bergisch Gladbach, Germany) was added, and the incubation continued for a further 4 days. They were then harvested and washed with phosphate-buffered saline (PBS) supplemented with 0.1 % FBS and 0.1 % NaN3. They were stained with allophycocyanin (APC)-CD3 (BD Bioscience) and 7-amino-actinomycin D (7-AAD; BD Bioscience). The proliferation of T cells was analyzed by the dilution of CFSE staining intensity using flow cytometry. Viable T cells were gated based on positive CD3 staining and negative 7-AAD staining. For blocking and neutralizing experiments, anti-B7H1 mAb and anti-B7DC mAb (each 10 μg/ml; eBioscience) and anti-TGF-β mAb and anti-VEGF mAb (each 10 μg/ml; R&D Systems) were used, respectively.

T cell apoptosis assay

A total of 500,000 PBMCs obtained from healthy donors were plated onto 48-well plates in culture supernatants from CAFs or NFs (half-diluted with conditioned RPMI 1640 medium). An anti-CD3/anti-CD28 stimulus was added and the incubation continued for a further 3 days. A CaspACE™ fluorescein isothiocyanate (FITC)-VAD-FMK In Situ Marker (Promega, Madison, WI, USA) was used to detect T cell apoptosis. After 3 days, PBMCs were harvested and washed with PBS supplemented with 0.1 % FBS and 0.1 % NaN3 and then stained with FITC-VAD-FMK according to the manufacturer's instructions. They were subsequently stained with APC-CD3 (BD Bioscience) and then analyzed by flow cytometry. Five microliters of 7-AAD was added prior to flow cytometry. T cells were gated based on positive CD3 staining.

Regulatory T cell induction assay

A total of 500,000 PBMCs obtained from healthy donors were plated onto 48-well plates in culture supernatants from CAFs or NFs (half-diluted with conditioned RPMI 1640 medium). An anti-CD3/anti-CD28 stimulus was added, and the incubation continued for a further 4 days. They were then harvested and washed with PBS supplemented with 0.1 % FBS and 0.1 % NaN3. To detect Foxp3+ regulatory T cells (Tregs), cells were stained with APC-CD4 antibodies (BD Bioscience), and intracellular staining for PE-Foxp3 (eBioscience) was then performed using a Cytofix/Cytoperm™ Kit and analyzed by flow

cytometry. Incubated PBMCs were harvested and washed with PBS and analyzed according to the method described in the real-time quantitative RT-PCR section. The relative mRNA expression levels of *FOXP3*, *IL10*, and *TGFB1* were examined.

Microarray analysis and pathway analysis

Three (CAF1/NF1, CAF2/NF2, and CAF3/NF3) of six pairs were compared using Agilent Whole Human Genome Oligo Microarrays (Agilent Technologies, Santa Clara, CA) according to the manufacturer's instructions. RNA was isolated using standard RNA extraction protocols (NucleoSpin RNA II, Macherey-Nagel, Germany), and qualified with a model of the 2100 Bioanalyzer (Agilent Technologies). All samples showed RNA Integrity Numbers of greater than 6.0 (9.9–10.0) and were subjected to microarray experiments. A hundred nanograms of the RNAs from NFs and CAFs were amplified and labeled with cyanine (Cy)3 and Cy5, respectively, using the Agilent Low Input Quick Amp Labeling kit (Agilent Technologies). The hybridization procedure was performed according to the Agilent 60-mer oligo microarray processing protocol using the Agilent Gene Expression Hybridization kit (Agilent Technologies). Briefly, 300 ng of the corresponding Cy3- and Cy5-labeled fragmented cRNA was combined and hybridized to the Agilent Whole Human Genome Oligo Microarray 8x60 k V2, and the fluorescence signals of the hybridized Agilent oligo microarrays were detected using Agilent's DNA microarray scanner (Agilent Technologies). The Agilent Feature Extraction Software was used to read out and process the microarray image files. The commonly upregulated genes (cutoff value, log 10 (ratio) > 0.5) in the three pairs were used for the pathway analysis using Ingenuity Pathway Analysis (IPA) software (Ingenuity Systems).

Statistical analysis

The Wilcoxon signed-rank test was used to test for differences in the means between two groups. Two-sided *P* values <0.05 were considered to be significant. All statistical analyses were performed using the Statistical Package for the Social Sciences version 22.0 (SPSS, Armonk, NY).

Results

Establishment of CAFs and NFs from HNSCC

Six pairs of CAFs and NFs were generated from the resected tumor samples of patients with HNSCC. These cells grew in primary cultures in an adherent fashion and possessed a fibroblast-like morphology. To confirm that these cells were fibroblasts, and not contaminated with leukocytes, endothelial cells, and tumor cells, cells were analyzed using flow cytometry. As shown in Fig. 1a, NFs and CAFs were both negative for CD11b, CD34, and CD45, and positive for CD90 and FAP, which indicated that they were not contaminated by any other cells. The levels of α-SMA expressed by CAFs were higher than those by NFs, indicating that fibroblasts prepared from tumor tissues possessed an activated phenotype. These results confirmed the identity of the cultures as CAFs and NFs for further assays.

Expression of HLA molecules and co-regulatory molecules on CAFs and NFs

The expression of HLA molecules and B7 family co-regulatory molecules was investigated to characterize the immunological phenotypes of CAFs and NF. CAFs and NFs were both positive for HLA class I, but not for HLA-DR, and the expression level of HLA class I was similar between CAFs and NFs (data not shown). As shown in Fig. 1b, CAFs and NFs were both negative for CD80, CD86, and B7H3. Furthermore, CAFs, but not NFs, expressed B7H1 and B7DC on the cell surface; however, the expression level of B7H1 and B7DC on CAFs was modest.

Up-regulation of cytokine genes in CAFs

We analyzed differences in the expression levels of various cytokine genes, including *IL6*, *CXCL8*, *TNF*, *TGFB1*, and *VEGFA*, between CAFs and NFs by real-time quantitative RT-PCR. The expression levels of the cytokine genes tested were higher in CAFs obtained from six HNSCC patients than in control NFs (Fig. 1c). Their increasing ratio of gene expression varied with each cytokine or in each case.

Inhibition of T cell proliferation

To assess the effects of CAFs and NFs on T cell proliferation, CAFs and NFs were co-cultured with CFSE-labeled T cells. After 4 days of being co-cultured with the anti-CD3/anti-CD28 stimulus, the proliferation of T cells was measured using flow cytometry. In co-cultures, the suppressor activity of CAFs was greater than that of NFs (Fig. 2a). In order to confirm whether CAFs suppressed T cell proliferation in a cell contact-dependent or cytokine-dependent manner, the culture supernatant from CAFs was harvested and used instead of CAFs in the T cell proliferation assay. As expected, the inhibition of T cell proliferation by the culture supernatant from CAFs was higher than that from NFs (Fig. 2b). Moreover, as shown in Fig. 2c, in six HNSCC patients tested, the culture supernatant from CAFs showed greater suppressor activity than that from NFs. These results suggested that CAFs directly suppressed

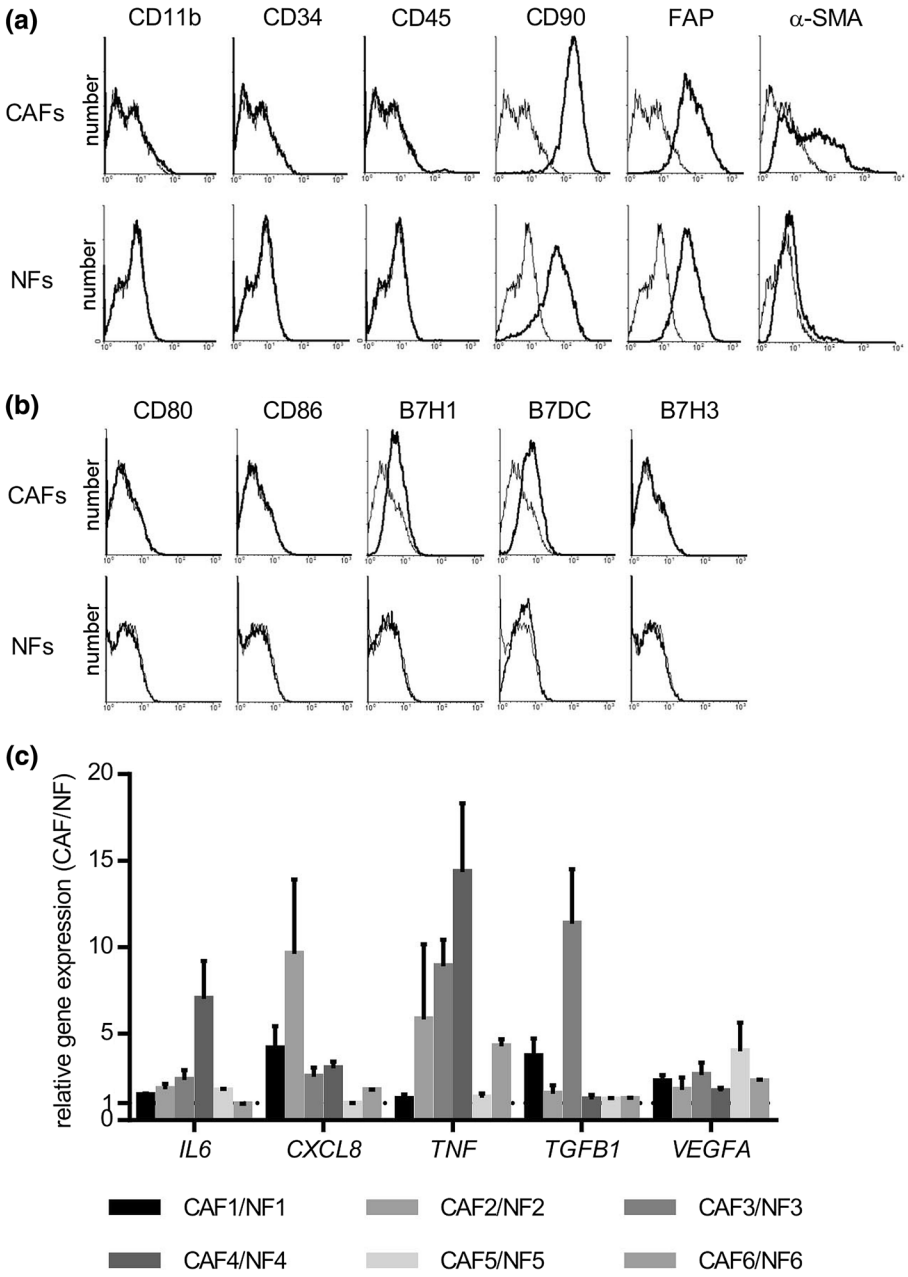

Fig. 1 Establishment of CAFs and NFs from HNSCC and their characteristics. Flow cytometry analysis of CAFs and NFs generated from resected tumor samples of patients with HNSCC. Primary cultures of CAFs and NFs were stained with CD11b, CD34, CD45, CD90, FAP, and α-SMA. CAFs and NFs were both negative for CD11b, CD34, and CD45, and positive for CD90 and FAP. α-SMA expression levels in CAFs were higher than those in NFs. **a** Representative data from one cancer patient. The expression of co-stimulatory and co-regulatory molecules on CAFs and NFs. Flow cytometry was performed as described in the "Materials and methods" section. **b** Representative data from one cancer patient. CAFs and NFs were both negative for CD80, CD86, and B7H3. The expression levels of B7H1 and B7DC in CAFs were higher than those in NFs. Up-regulation of cytokine genes in CAFs from HNSCC patients. **c** Total RNA was extracted from the generated CAFs and NFs, and increases in the expression levels of *IL6*, *CXCL8*, *TNF*, *TGFB1*, and/or *VEGFA* were detected by real-time qRT-PCR

anti-tumor immune responses by producing various soluble factors including immunosuppressive cytokines.

Inhibitory mechanisms of T cell proliferation by CAFs

Next, the potential role of co-regulatory molecules and immunosuppressive cytokines in the suppressive function of CAFs was investigated through the use of mAbs. As expected, addition of anti-B7H1 mAb and anti-B7DC mAb significantly restored T cell proliferation (Fig. 3a, b). Thus, the suppressive effects of CAFs appear to be partially mediated by co-regulatory molecules. These results suggested that CAFs had different immunological properties to NFs. Similarly, we investigated the importance of two immunosuppressive cytokines, TGF-β and VEGF, as key molecules suppressing T cell proliferation. To end this, we neutralized TGF-β and VEGF from supernatants of CAFs using antibodies. As shown in Fig. 3c, d, neutralizing TGF-β and VEGF led to an increase of proliferated T cells. These findings suggest a pivotal role of TGF-β and VEGF as soluble factors in immune suppression mediated by CAFs.

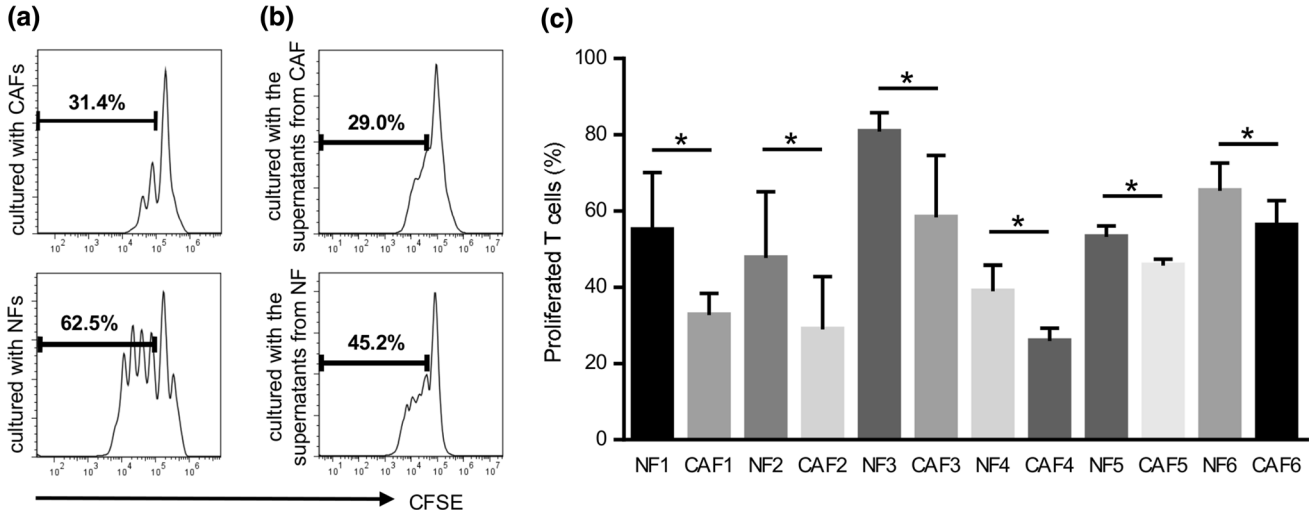

Fig. 2 Suppressive activity on T cell proliferation by CAFs and NFs. Generated CAFs and NFs were co-cultured with CFSE-labeled T cells for 4 days with an anti-CD3/anti-CD28 stimulus. They were stained with APC-CD3 and 7-amino-actinomycin D (7-AAD) to gate viable CD3+ T cells. The proliferation of T cells was analyzed by the reduction of CFSE staining intensity using flow cytometry. **a** Representative data of the proliferation of T cells cultured with CAFs or NFs. **b** Representative data of the proliferation of T cells cultured with supernatants from CAFs or NFs. **c** The culture supernatant from CAFs showed greater suppressor activity than that from NFs in six HNSCC patients tested. Bars indicate mean values derived from 6 independent experiments. *Asterisk* indicates significant difference ($P < 0.05$) between NFs and CAFs

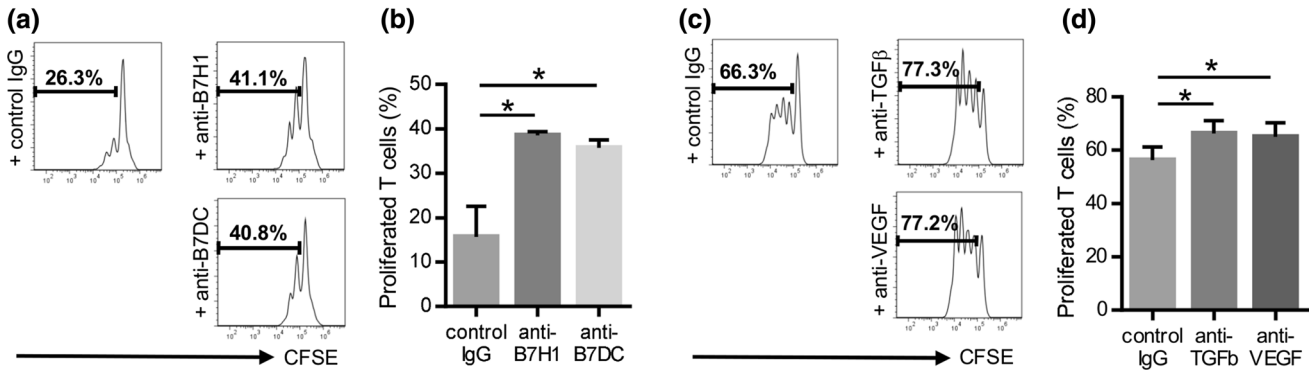

Fig. 3 Role of co-regulatory molecules and immunosuppressive cytokines in T cell suppression by CAFs. CAFs were pretreated with anti-B7H1 mAb or anti-B7DC mAb, and then co-cultured with CFSE-labeled T cells for 4 days with an anti-CD3/anti-CD28 stimulus. The proliferation of T cells was analyzed using flow cytometry. **a** Representative data from one patient (CAF5). **b** Addition of anti-B7H1 mAb and anti-B7DC mAb significantly restored T cell proliferation. Similarly, CAFs supernatants were pretreated with anti-TGF-β or anti-VEGF neutralizing mAb, and then added to CFSE-labeled PBMCs for T cell proliferation assays. **c** Representative data from one patient (CAF3). **d** TGF-β and VEGF neutralization also significantly increased the percentage of proliferated T cells. *Asterisk* indicates significant difference ($P < 0.05$) compared with control IgG

Induction of T cell apoptosis

To further elucidate the mechanisms underlying the suppression of T cell proliferation, we investigated whether the culture supernatants obtained from CAFs and NFs induced T cell apoptosis. Healthy donor PBMCs were cultured with supernatants from CAFs or NFs for 3 days with an anti-CD3/anti-CD28 stimulus, and were subsequently analyzed by flow cytometry. The proportions of apoptotic T cells in PBMCs co-cultured with the supernatant from CAFs were significantly higher than those co-cultured with the supernatant from NFs (Fig. 4a, b).

Induction of regulatory T (Treg) cells

We compared the percentages of Treg cells in PBMCs co-cultured with supernatant obtained from CAFs or NFs. Representative dot plots of Treg cells

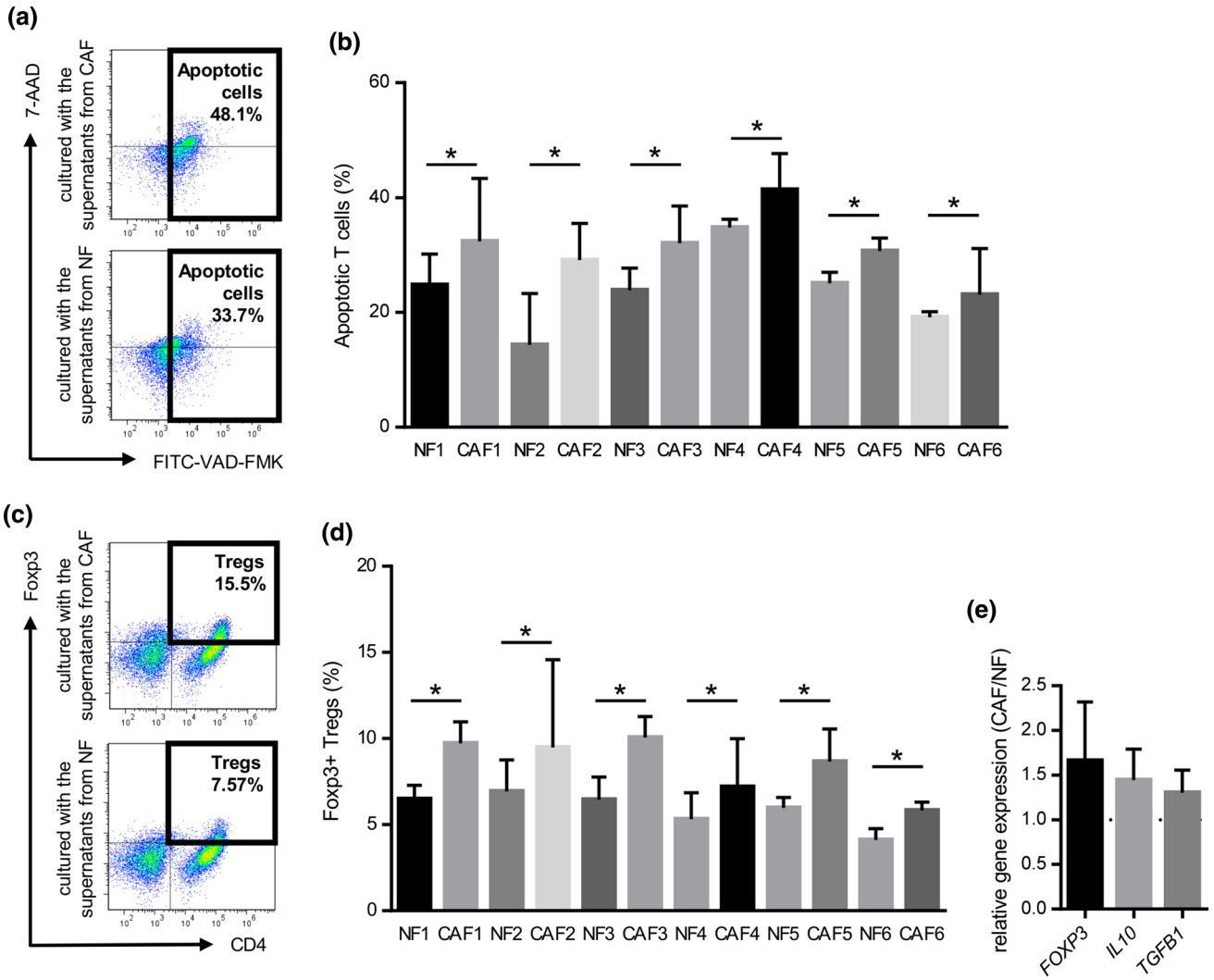

Fig. 4 Induction of T cell apoptosis and Treg (CD4+Foxp3+) in PBMCs co-cultured with the supernatant from CAFs or NFs. PBMCs prepared from healthy donors were cultured with the supernatant from CAFs or NFs for 3 days with an anti-CD3/anti-CD28 stimulus, and subsequently analyzed by flow cytometry. They were stained with FITC-VAD-FMK, APC-CD3, and 7-amino-actinomycin D (7-AAD), and CD3+ T cells were gated. **a** Representative data of apoptotic T cells cultured with CAFs or NFs. **b** The induction of T cell apoptosis was significantly greater by CAFs from the six HNSCC patients tested than by NFs. Bars indicate mean values derived from 6 independent experiments. *Asterisk* indicates significant difference ($P < 0.05$) between NFs and CAFs. PBMCs prepared from healthy donors were co-cultured with the supernatant from CAFs or NFs for 4 days with an anti-CD3/anti-CD28 stimulus. They were stained with PE-Foxp3 and APC-CD4, and then analyzed by flow cytometry. They were also analyzed by real-time qRT-PCR after a 3-day incubation. **c** Representative data of CD4+Foxp3+Tregs in PBMCs co-cultured with the supernatant from CAFs or NFs. **d** The induction of T reg was significantly greater by CAFs from the six HNSCC patients tested than by NFs. Bars indicate mean values derived from 6 independent experiments. *Asterisk* indicates significant difference ($P < 0.05$) between NFs and CAFs. **e** The expression levels of Treg-related genes including *FOXP3*, *TGFB1*, and *IL10* in PBMCs co-cultured with the supernatant from CAFs was higher than those co-cultured with the supernatant from with NFs

(CD4+FOXP3+) are shown in Fig. 4c. As expected, the proportions of Treg cells in PBMCs co-cultured with the supernatant obtained from CAFs were significantly higher than those co-cultured with the supernatant from NFs (Fig. 4d). Moreover, the gene expression levels of the Treg-specific transcription factors *FOXP3*, *IL-10*, and *TGFB1* in PBMCs co-cultured with supernatant were analyzed by real-time quantitative RT-PCR, and the expression levels of *FOXP3*, *IL10*, and *TGFB1* were higher in PBMCs co-cultured with supernatant obtained from CAFs than in those co-cultured with the supernatant from NFs (Fig. 4e). These results suggested that CAFs also indirectly suppressed anti-tumor immune responses by inducing Treg cells.

Microarray analysis and pathway analysis

We performed Agilent Whole Human Genome Microarray analyses with the three pairs of CAFs and NFs. Although a hierarchical cluster analysis from the three (CAF1/NF1, CAF2/NF2, and CAF3/NF3) of six pairs revealed different genetic profiles, as shown in Fig. 5a, a hundred genes that were upregulated in the three CAFs (log 10 ratio > 0.5) were identified (Fig. 5b). To explore the altered canonical pathways in CAFs from those in NFs, we characterized the functional relationship between genes upregulated in CAFs in IPA. Two signaling pathways, the leukocyte extravasation and paxillin signaling pathways, have been predicted as the most significantly activated canonical pathways (Table 1).

Discussion

Anti-tumor immunity has been considered to play an important role in protecting against the development of malignancy. The immune system monitors and excludes tumor cells in the early phase of tumorigenesis, and fibroblasts also contribute to a growth suppressive state, while tumor cell variants show increased resistance to immune surveillance and gradually survive and proliferate. Immune responses against tumor cells in the TME were previously reported to be strongly suppressed through a dysfunction in effector cells, as well as the infiltration and expansion of immune suppressive cells, and where fibroblasts educated by tumor cells become CAFs contributing to tumorigenesis, tumor growth, and metastasis [5, 9]. Regarding the contribution of CAFs to immune evasion, Balsamo et al. [17] demonstrated that CAFs from melanoma interfered with NK cell functions including cytotoxicity and cytokine production. On the other hand, De Monte et al. [18] reported that CAFs from pancreatic cancer induced thymic stromal lymphopoietin-dependent Th2-type inflammation. In addition to these findings, we were able to demonstrate in the present study that CAFs obtained from HNSCC were of unique immunological significance, as opposed to NFs.

Our results revealed that CAFs suppressed T cell proliferation more efficiently than NFs. This suppressive activity was observed in co-cultures not only with CAFs, but also the supernatant from CAFs. To elucidate the mechanisms underlying the suppressive effects of CAFs on T cell proliferation, we first assessed the expression of co-stimulatory and co-regulatory molecules by CAFs and NFs. Although co-stimulatory molecules, CD80 and CD86, were not expressed by CAFs or NFs, B7H1 and B7DC were expressed by CAFs, but not by NFs. B7H1 and B7DC are both members of the B7 family, bind PD-1 on activating T cells, and are putative negative regulators for immune function. Nazareth et al. [19] demonstrated that a subset of CAFs obtained from non-small cell lung cancer (NSCLC) constitutively expressed B7H1 and B7DC. The intensity of B7H1/B7DC expression in CAFs from HNSCC was more modest than that in CAFs obtained from NSCLC. We performed blocking assays using anti-B7H1 and anti-B7DC mAbs, and suppressive activity was significantly restored in some of pairs tested. Nazareth et al. showed that the blockade of B7H1 and/or B7DC completely reversed the inhibition of tumor-associated T cell activation by CAFs in one of three tumors. Thus, our results and previous findings suggest that co-regulatory molecules on CAFs may partially play an important role in T cell suppression. CAFs originally consist of a heterogeneous population of cells from various sources; therefore, the role of B7H1 and B7/DC expression in CAFs may vary depending on factors such as their functional activities, types of cancers, and immune status in the TME. Several monoclonal antibodies that target B7H1 (PD-L1) are now being developed [20, 21], and the blockade of B7H1 was recently shown to produce durable tumor regression and prolonged disease stabilization in patients with advanced cancers in a phase I trial [22]. Monoclonal antibodies against co-regulatory molecules may be somewhat useful as a CAF-targeted therapy.

Since CAFs suppressed T cell proliferation in a contact-independent manner, we investigated T cell apoptosis and Treg induction using culture supernatants from CAFs and NFs in order to elucidate the suppression mechanisms responsible in more detail. Previous studies have so far demonstrated that CAFs produce various cytokines and/or chemokines to promote tumor cell proliferation, angiogenesis, invasion, and metastatic dissemination [9]. Several studies found that CAFs isolated from HNSCC expressed higher levels of hepatocyte growth factor (HGF) [23], TGF-β [24], IL-33 [25], chemokine ligand 7 (CCL7) [26], and matrix metalloproteinase (MMP) [27] than their normal counterparts. We also revealed that the gene expression levels of *IL6*, *CXCL8*, *TNF*, *TGFB1*, and *VEGFA* were higher in CAFs than in NFs. Among the cytokines evaluated in the present study, TNF-α is known to be a member of cytokines that induce apoptotic cell death in T cells. Therefore, it was not unexpected to find that CAFs significantly induced T cell apoptosis; however, difficulties have been associated with determining the exact factors involved in T cell apoptosis due to its complicated composition. PBMCs co-cultured with the supernatant from CAFs preferentially induced Treg. Moreover, the gene expression levels of *FOXP3*, *TGFB1*, and *IL10* were elevated in PBMCs co-cultured with the supernatant from CAFs, which supported the induced Treg being functionally activated. Treg has been shown to accumulate in the TME, promote tumor growth, and down-regulate anti-tumor responses [28]. The differentiation of precursor T cells is regulated by a complex network of specific cytokine signals, and a certain type of Treg is known to be induced in the

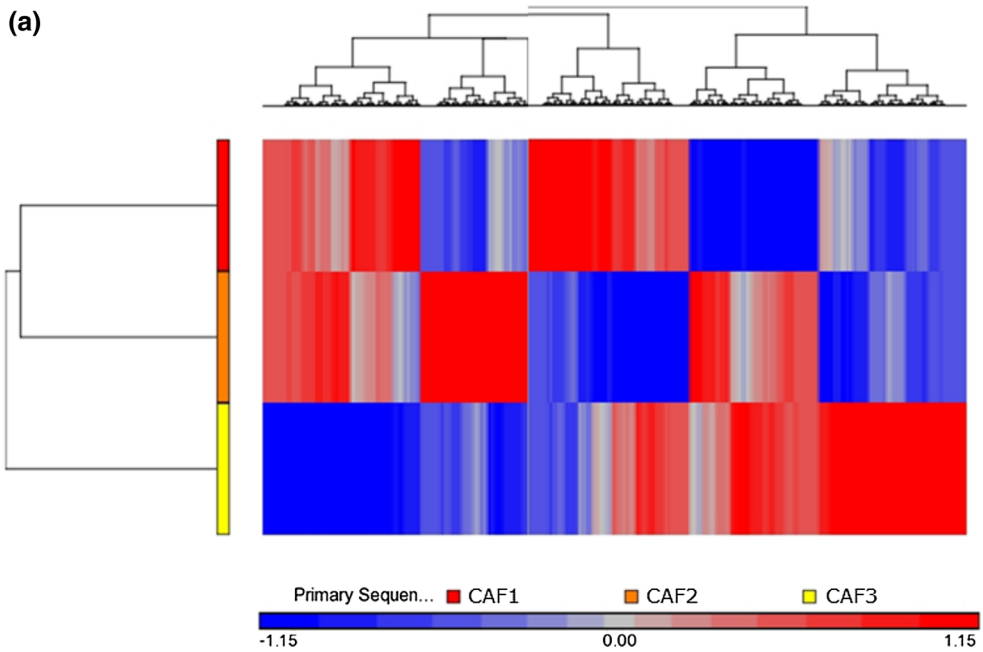

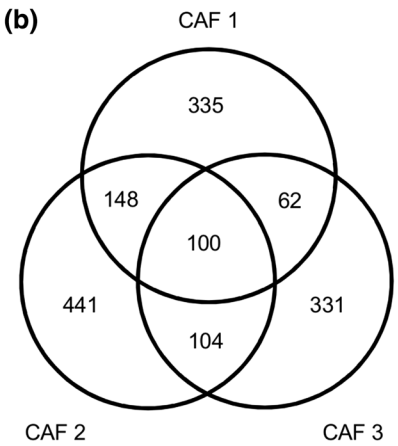

ST6GALNAC5	*IL17F*	*PDZRN4*	*MBOAT1*	*PROC*
NFE2L3	*BST2*	*COL8A1*	*TFAP2A*	*NXPH2*
APCDD1	*RAB38*	*DMD*	*CD163L1*	*PLCB4*
TNFSF4	*TRPA1*	*GPR65*	*ADAMTS12*	*SLC24A4*
WFDC1	*STRA6*	*FAM169A*	*PAGE3*	*RNF144B*
VAT1L	*MAMDC2*	*COLEC10*	*CLDN18*	*MIR143HG*
SLC24A3	*OR10A7*	*MC5R*	*VWC2L*	*VPREB3*
RUNX3	*NEDD9*	*OR9G4*	*PSG1*	*KIAA0408*
LEF1	*ITGA1*	*SGIP1*	*CLDN1*	*ITGA4*
C7orf69	*TMEM176B*	*PYY*	*GREB1L*	*STYK1*
COL10A1	*B3GALT2*	*DMRT1*	*LINC00483*	*FRY*
BEX1	*ELOVL2*	*LINC00460*	*PSG8*	*NRXN1*
EFNB2	*CHN1*	*RASGRP1*	*FOLH1*	*PNKD*
NTF3	*AZU1*	*CLEC1A*	*CD8A*	*LINC00161*
FAM155A	*MMP1*	*HCLS1*	*TNS3*	*LRRC38*
HSPA2	*PADI1*	*MRVI1*	*SHROOM2*	*BCL11B*
PTPRB	*MMP3*	*A2M*	*LYPD6*	*H2AFB3*
RASEF	*SNCAIP*	*FRZB*	*CNN1*	*AGAP6*
OXTR	*DKK2*	*ANGPT1*	*FGF1*	*LINC00862*
EML5	*FAM84A*	*FAM101A*	*PIK3R3*	*RGCC*

Fig. 5 Microarray analyses with the three pairs of CAFs and NFs. **a** Cluster diagram of a microarray analysis from three pairs of NFs and CAFs. The color bar estimates relative expression levels: *Red* indicates higher than average expression and blue indicates lower than average expression. **b** A list of commonly upregulated genes in CAFs obtained from three patients with HNSCC. A total of one hundred genes were identified as commonly upregulated genes from the microarray analysis between NFs and CAFs. The cutoff value of the log 10 (ratio) was set to be greater than 0.5

periphery in response to IL-2, TGF-β, and IL-10 [29]. Moreover, VEGF has been recognized as an important factor in the induction or maintenance of Treg [30]. The up-regulation of *TGFB1* and *VEGFA* in CAFs may play an important role in the induction of Treg. In fact, restoration of T cell proliferation by TGF-β and VEGF neutralization in the present

Table 1 List of genes in significantly upregulated canonical pathways identified by IPA

Ingenuity canonical pathways	Sample	−log (*P* value)	Ratio	z-Score	Molecules
Leukocyte extravasation signaling	Pt-1	5.70	0.104	3.5	*RAC2,VCAM1,ICAM1,MMP3,ACTN3,CLDN18,ITGA6,ITGB3, PIK3R3, ITGB2,ITGA3,EDIL3,ARHGAP9, ACTA2,CLDN1,RASGRP1,ITGA1, CLDN9,MMP1,ITGA4*
	Pt-2	5.80	0.119	3.771	*MMP3,ACTB,ACTN3,CLDN18, ITGA6,PIK3R3,ITGB2,CLDN24, ITGA3,EDIL3,ACTA2,ARHGAP9, CLDN1,PLCG2,RASGRP1,ITGA1, ACTG2,CLDN9,MMP12,ACTN1, MMP1,ATM,ITGA4*
	Pt-3	4.51	0.088	3.317	*CLDN11,SPN,MMP3,CLDN18,JAM2,MMP25,CLDN6,MMP27 ,PIK3R3, CLDN1,RASGRP1,PIK3R6,ITGA1, ACTG2,MMP12,MMP1,ITGA4*
Paxillin signaling	Pt-1	2.51	0.092	2.236	*PIK3R3,ITGB2,ITGA3,ACTA2, ACTN3,ITGA6,ITGA1,ITGA4,ITGB3*
	Pt-2	3.42	0.122	3	*PIK3R3,ITGB2,ITGA3,ACTA2,ACTB,ACTN3,ITGA6,ITGA1,A CTG2, ACTN1,ITGA4,ATM*
	Pt-3	1.70	0.071	2.449	*PIK3R3,PAK3,ARHGEF7,PIK3R6, ITGA1,ACTG2,ITGA4*

study supports that. Mace et al. [31] similarly demonstrated that a culture of PBMCs with pancreatic cancer stellate cell supernatants promoted PBMC differentiation into myeloid-derived suppressor cells, which is another major subset of regulatory cells, in a STAT3-dependent manner. Thus, various factors secreted by CAFs appear to act synergistically or additively to enhance immunosuppressive ability, leading to a dysfunction in effector T cells.

We also compared the gene expression profiles of CAFs and NFs using a microarray analysis. The hierarchical clustering of gene expression in CAFs than in NFs clearly showed differences between individual patients. These results suggest that the characteristics of CAFs in the TME may be regulated by various conditions, such as inflammation, hypoxia, and angiogenesis, in which CAFs exist. In order to elucidate the activated signaling pathway related to CAFs, commonly upregulated genes in the three pairs were analyzed with IPA. Although any signaling pathway related to immunosuppression was not detected in this study, we additionally found that a set of genes, the expression of which was upregulated in CAFs, were involved in the leukocyte extravasation and paxillin signaling pathways. Paxillin is one of the crucial molecules for cell–extracellular matrix adhesion and cell migration, and plays an important role in the assembly and disassembly of focal adhesions in various cells [32, 33]. These activated signaling pathways in CAFs may facilitate the recruitment of various leukocytes including immunosuppressive cells in the TME.

In summary, we established pairs of CAFs and NFs from patients with HNSCC. CAFs expressed not only the co-regulatory molecules, B7H1 and B7DC, but also preferentially induced T cell apoptosis and Treg over NFs. Moreover, the leukocyte extravasation and paxillin signaling pathways were predicted to be the most significantly activated canonical pathways in CAFs relative to those in NFs. Thus, CAFs modulated effector T cell function in anti-tumor immune responses in direct and indirect manners. Tumor evasion from the host immune system is a major problem in immunotherapy, and CAFs may play a pivotal role in the TME by establishing an immunosuppressive network along with tumor cells and immunosuppressive cells that facilitates the activation of an immunosuppressive pathway. Accordingly, the development of novel therapeutic agents to efficiently overcome CAF-driven immunosuppression is urgently needed.

Acknowledgments This work was supported in part by KAKENHI (Grants-in-Aid for Scientific Research) (15K10798 to Koichi Sakakura, 25861525 to Minoru Toyoda, 26670736 to Kazuaki Chikamatsu). We thank Dr. Theresa L. Whiteside for her critical reading and comments.

Compliance with ethical standards

Conflict of interest The authors declare that they have no conflict of interest.

References

1. Siegel R, Naishandham D, Jemal A (2012) Cancer statistics, 2012. CA Cancer J Clin 62:10–29

2. Leemans CR, Braakhuis BJM, Brakenhoff RH (2011) The molecular biology of head and neck cancer. Nat Rev Cancer 11:9–22
3. Augsten M (2014) Cancer-associated fibroblasts as another polarized cell type of the tumor microenvironment. Front Oncol 4:62
4. Franco OE, Shaw AK, Strand DW, Hayward SW (2010) Cancer associated fibroblasts in cancer pathogenesis. Semin Cell Dev Biol 21:33–39
5. Kalluri R, Zeisberg M (2006) Fibroblasts in cancer. Nat Rev Cancer 6:392–401
6. Ito M, Ishii G, Nagai K, Maeda R, Nakano Y, Ochiai A (2012) Prognostic impact of cancer-associated stromal cells in patients with stage I lung adenocarcinoma. Chest 142:151–158
7. Herrera M, Herrera A, Domínguez G, Silva J, García V, García JM, Gómez I, Soldevilla B, Muñoz C, Provencio M, Campos-Martin Y, García de Herreros A et al (2013) Cancer-associated fibroblast and M2 macrophage markers together predict outcome in colorectal cancer patients. Cancer Sci 104:437–444
8. Zhang J, Liu J (2013) Tumor stroma as targets for cancer therapy. Pharmacol Ther 137:200–215
9. Rasanen K, Vaheri A (2010) Activation of fibroblasts in cancer stroma. Exp Cell Res 316:2713–2722
10. Zhang L, Conejo-Garcia JR, Katsaros D, Gimotty PA, Massobrio M, Regnani G, Makrigiannakis A, Gray H, Schlienger K, Liebman MN, Rubin SC, Coukos G (2003) Intratumoral T cells, recurrence, and survival in epithelial ovarian cancer. N Engl J Med 348:203–213
11. Pages F, Berger A, Camus M, Sanchez-Cabo F, Costes A, Molidor R, Mlecnik B, Kirilovsky A, Nilsson M, Damotte D, Meatchi T, Bruneval P et al (2005) Effector memory T cells, early metastasis, and survival in colorectal cancer. N Engl J Med 353:2654–2666
12. Whiteside TL (2010) Immune responses to malignancies. J Allergy Clin Immunol 125:S272–S283
13. Talmadge JE (2011) Immune cell infiltration of primary and metastatic lesions: mechanisms and clinical impact. Semin Cancer Biol 21:131–138
14. Poschke I, Mougiakakos D, Kiessling R (2011) Camouflage and sabotage: tumor escape from the immune system. Cancer Immunol Immunother 60:1161–1171
15. Hanahan D, Weinberg RA (2011) Hallmarks of cancer: the next generation. Cell 144:646–674
16. Tong CCL, Kao J, Silora AG (2012) Recognizing and reversing the immunosuppressive tumor microenvironment of head and neck cancer. Immunol Res 54:266–274
17. Balsamo M, Scordamaglia F, Pietra G, Manzini C, Cantoni C, Boitano M, Queirolo P, Vermi W, Facchetti F, Moretta A, Moretta L, Mingari MC et al (2009) Melanoma-associated fibroblasts modulate NK cell phenotype and antitumor cytotoxicity. Proc Natl Acad Sci USA 106:20847–20852
18. De Monte L, Reni M, Tassi E, Clavenna D, Papa I, Recalde H, Braga M, Di Carlo V, Doglioni C, Protti MP (2011) Intratumor T helper type 2 cell infiltrate correlates with cancer-associated fibroblast thymic stromal lymphopoietin production and reduced survival in pancreatic cancer. J Exp Med 208:469–478
19. Nazareth MR, Broderick L, Simpson-Abelson MR, Kelleher RJ Jr, Yokota SJ, Bankert RB (2007) Characterization of human lung tumor-associated fibroblasts and their ability to modulate the activation of tumor-associated T cells. J Immunol 178:5552–5562
20. Kyi C, Postow MA (2014) Checkpoint blocking antibodies in cancer immunotherapy. FEBS Lett 588:368–376
21. Hamid O, Carvajal RD (2013) Anti-programmed death-1 and anti-programmed death-ligand 1 antibodies in cancer therapy. Expert Opin Biol Ther 13:847–861
22. Brahmer JR, Tykodi SS, Chow LQ, Hwu WJ, Topalian SL, Hwu P, Drake CG, Camacho LH, Kauh J, Odunsi K, Pitot HC, Hamid O et al (2012) Safety and activity of anti-PD-L1 antibody in patients with advanced cancer. N Engl J Med 366:2455–2465
23. Knowles LM, Stabile LP, Egloff AM, Rothstein ME, Thomas SM, Gubish CT, Lerner EC, Seethala RR, Suzuki S, Quesnelle KM, Morgan S, Ferris RL et al (2009) HGF and c-Met participate in paracrine tumorigenic pathways in head and neck squamous cell cancer. Clin Cancer Res 15:3740–3750
24. Rosenthal E, McCrory A, Talbert M, Young G, Murphy-Ullrich J, Gladson C (2004) Elevated expression of TGF-β1 in head and neck cancer-associated fibroblasts. Mol Carcinog 40:116–121
25. Chen SF, Nieh S, Jao SW, Wu MZ, Liu CL, Chang YC, Lin YS (2013) The paracrine effect of cancer-associated fibroblast-induced interleukin-33 regulates the invasiveness of head and neck squamous cell carcinoma. J Pathol 231:180–189
26. Jung DW, Che ZM, Kim J, Kim K, Kim KY, Williams D, Kim J (2010) Tumor-stromal crosstalk in invasion of oral squamous cell carcinoma: a pivotal role of CCL7. Int J Cancer 127:332–344
27. Johansson AC, Ansell A, Jerhammar F, Lindh MB, Grenman R, Munck-Wikland E, Östman A, Roberg K (2012) Cancer-associated fibroblasts induce matrix metalloproteinase-mediated cetuximab resistance in head and neck squamous cell carcinoma cells. Mol Cancer Res 10:1158–1168
28. Elkord E, Alcantar-Orozco EM, Dovedi SJ, Tran DQ, Hawkins RE, Gilham DE (2010) T regulatory cells in cancer: recent advances and therapeutic potential. Expert Opin Biol Ther 10:1573–1586
29. Knosp CA, Johnston JA (2012) Regulation of CD4+ T-cell polarization by suppressor of cytokine signalling proteins. Immunology 135:101–111
30. Wada J, Suzuki H, Fuchino R, Yamasaki A, Nagai S, Yanai K, Koga K, Nakamura M, Tanaka M, Morisaki T, Katano M (2009) The contribution of vascular endothelial growth factor to the induction of regulatory T-cells in malignant effusions. Anticancer Res 29:881–888
31. Mace TA, Ameen Z, Collins A, Wojcik S, Mair M, Young GS, Fuchs JR, Eubank TD, Frankel WL, Bekaii-Saab T, Bloomston M, Lesinski GB (2013) Pancreatic cancer-associated stellate cells promote differentiation of myeloid-derived suppressor cells in a STAT3-dependent manner. Cancer Res 73:3007–3018
32. Gumbiner BM (1996) Cell adhesion: the molecular basis of tissue architecture and morphogenesis. Cell 84:345–357
33. Turner CE (2000) Paxillin and focal adhesion signaling. Nat Cell Biol 2:E231–E236